Supplementary information

Using smartphone APP to determine CN^{-} concentration quantitatively in tap water: synthesis of the naked-eye colorimetric chemosensor for CN^{-} and Ni^{2+} based on benzothiazole

Cui-Bing Bai,[†,‡] Xin-Yu Liu,[†] Jie Zhang,[†] Rui Qiao,*[,†,‡] Kun Dang,[†] Chang Wang,[†,‡] Biao Wei,[†,‡] Lin Zhang,[†,‡] Shui-Sheng Chen[†,‡]

[†] School of Chemistry and Materials Engineering, Fuyang Normal University, Fuyang, Anhui Province, 236037, China.

[‡] Engineering Research Center of Biomass Conversion and Pollution Prevention of Anhui Educational Institutions, Fuyang Normal University, Fuyang, Anhui Province, 236037, China

** Corresponding Author E-mail: qiaorui@mail.ipc.ac.cn*

Contents

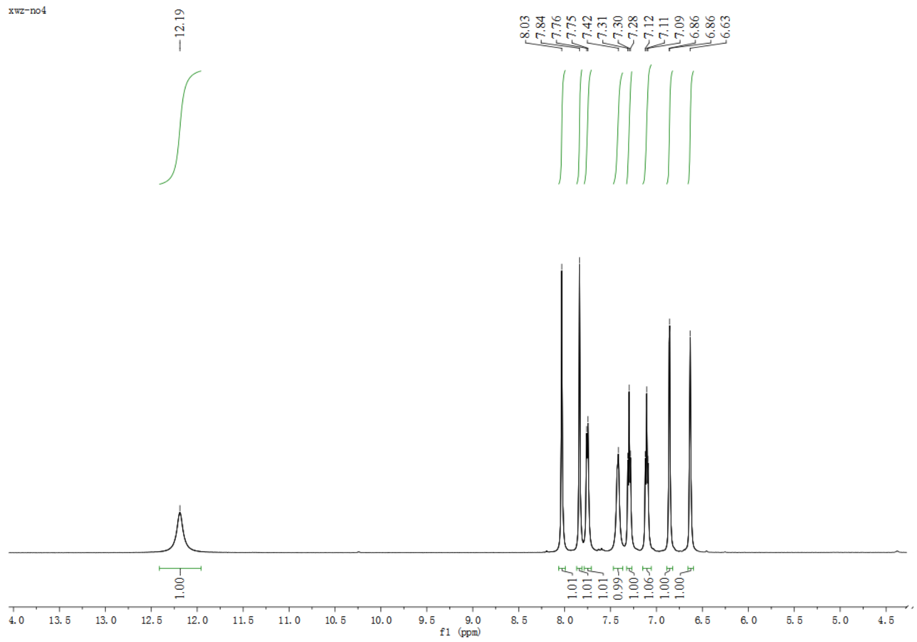

Figure S1 ^{1}H NMR spectrum of **DK** in DMSO-d_6.

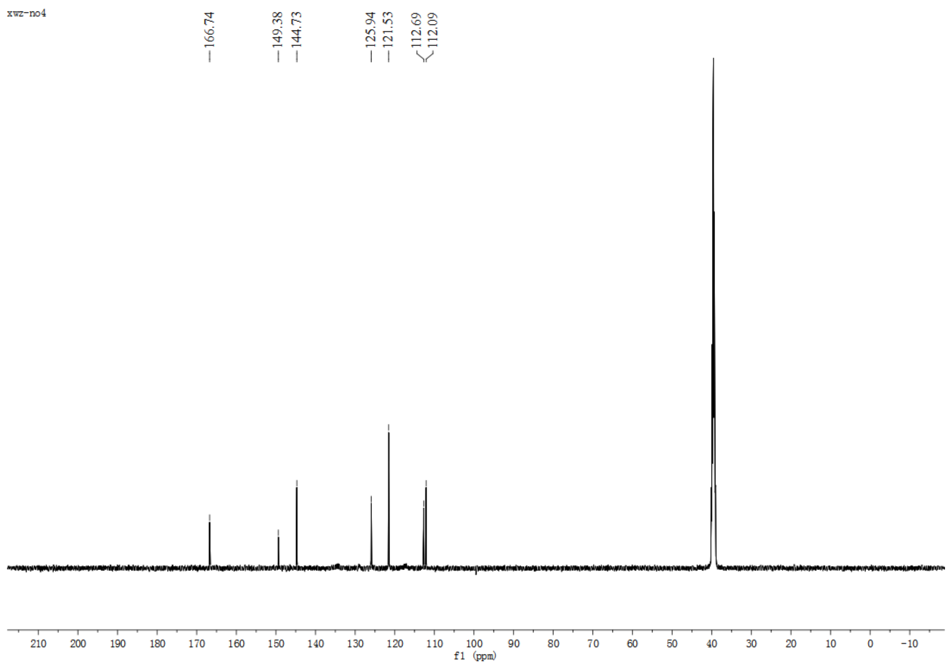

Figure S2 ^{13}CNMR spectrum of **DK** in DMSO-d_6.

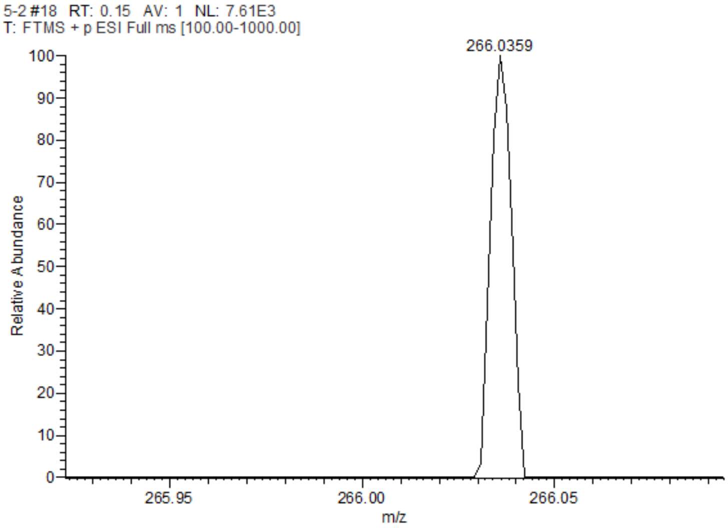

Figure S3 ESI-MS spectrum of **DK**.

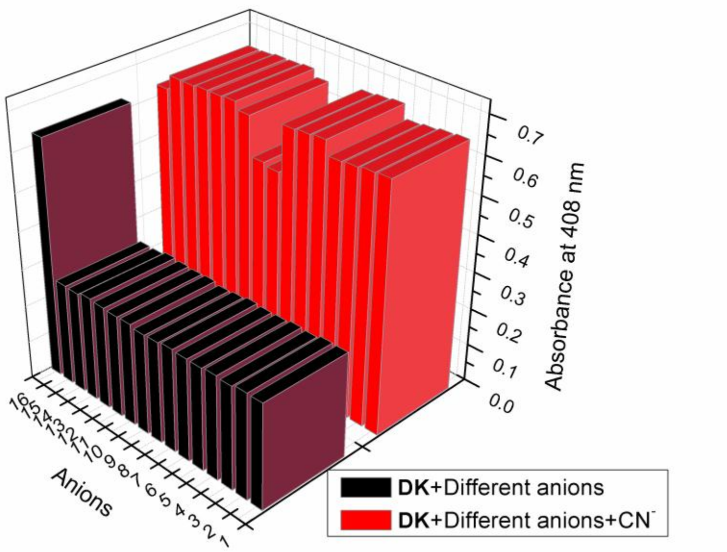

Figure S4 Black bar: Absorption spectra of **DK** with different anions in HEPES buffer /CH_3CN (0.01 M, pH=7.3, V/V = 10:90) solution. Red bar: Absorption spectra of **DK** with the mixture of CN^- and other anions in HEPES buffer /CH_3CN (0.01 M, pH=7.3, V/V = 10:90) solution. 1-16: F^-, Cl^-, Br^-, I^-, SO_4^{2-}, SO_3^{2-}, S^{2-}, NO_3^-, NO_2^-, PO_4^{3-}, CO_3^{2-}, HCO_3^-, AcO^-, EDTA, $H_2PO_4^-$, CN^-.

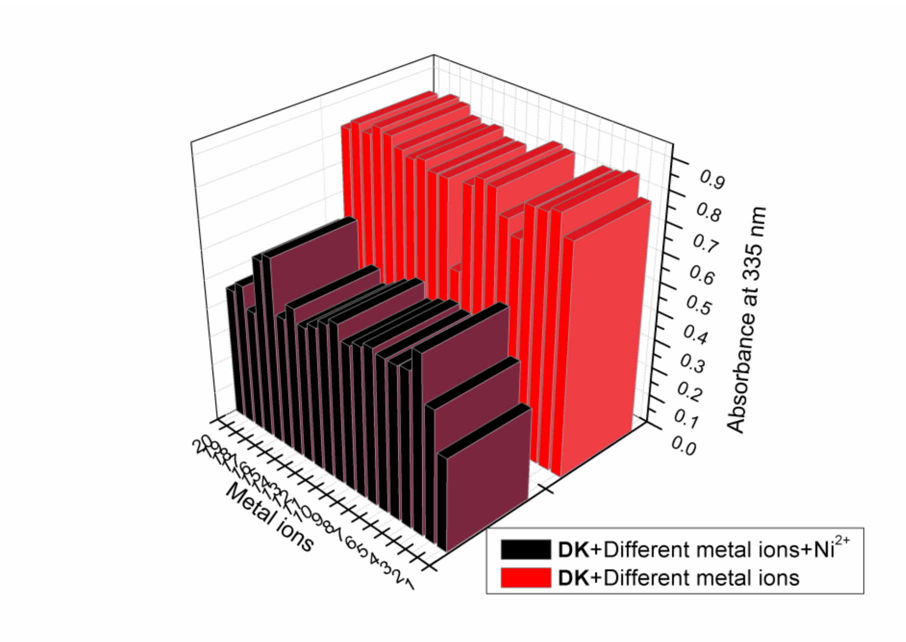

Figure S5 Black bar: Absorption spectra of **DK** with the mixture of Ni^{2+} and other metal ions in HEPES buffer /CH_3CN (0.01 M, pH=7.3, V/V = 10:90) solution. Red bar: Absorption spectra of **DK** with different metal ions in HEPES buffer /CH_3CN (0.01 M, pH=7.3, V/V = 10:90) solution. 1-20: Fe^{2+}, Fe^{3+}, Hg^{2+}, Na^{+}, Cu^{2+}, Co^{2+}, Mg^{2+}, Ce^{3+}, Cd^{2+}, Ni^{2+}, Zn^{2+}, Ag^{+}, K^{+}, Ba^{2+}, Pb^{2+}, Y^{3+}, Al^{3+}, Sr^{2+}, Mn^{2+}, Ca^{2+}.

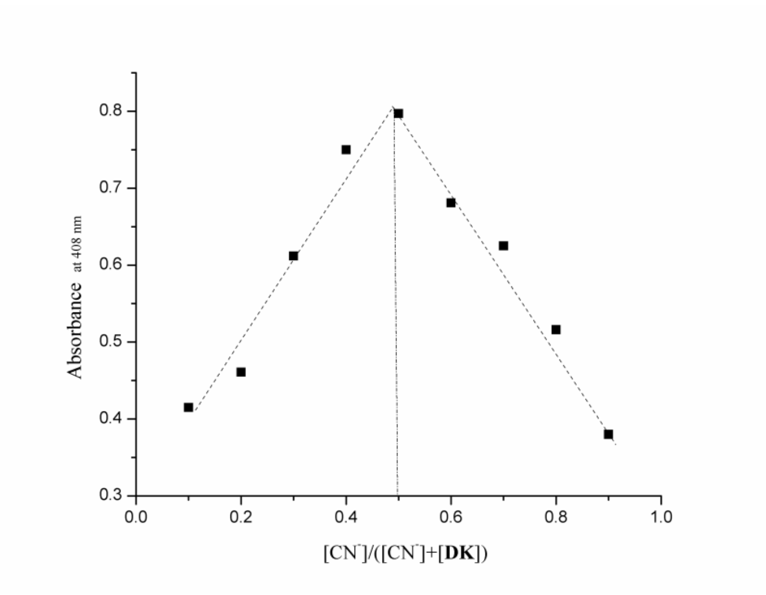

Figure S6 A Job's plot for the **DK** and CN^{-} based oncontinuous variation method.

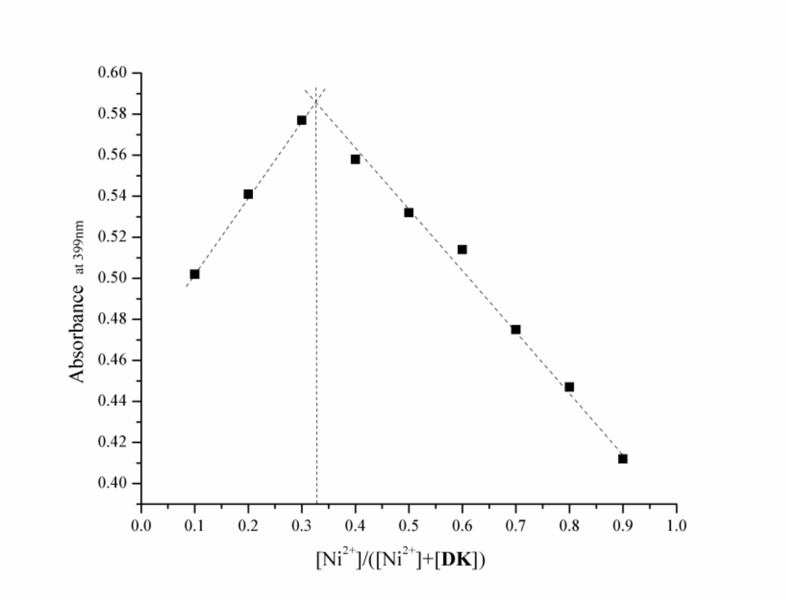

Figure S7 A Job's plot for the **DK** and Ni^{2+} based oncontinuous variation method.

(a)

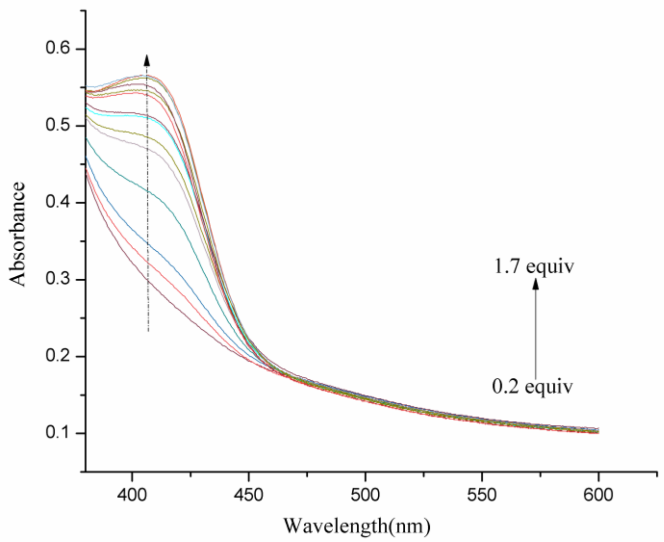

(b)

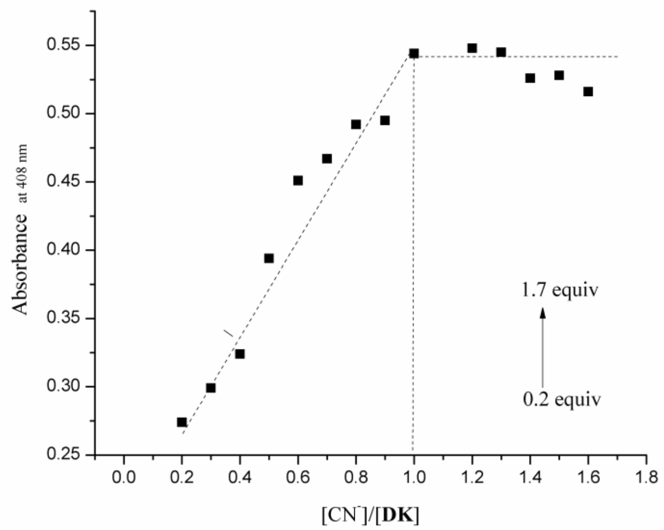

Figure S8 Job's Plot showing the 1:1 stoichiometry between **DK** and CN^-. (a) Absorption spectra of **DK** (1.0×10^{-5} M) in the presence of different concentration of CN^- (0.2-1.7 equiv.) in HEPES buffer /CH_3CN (0.01 M, pH=7.3, V/V = 10:90) solution. (b) A plot of absorption intensity depending on the concentration of CN^- in the range from 0.2-1.7 equiv.

(a)

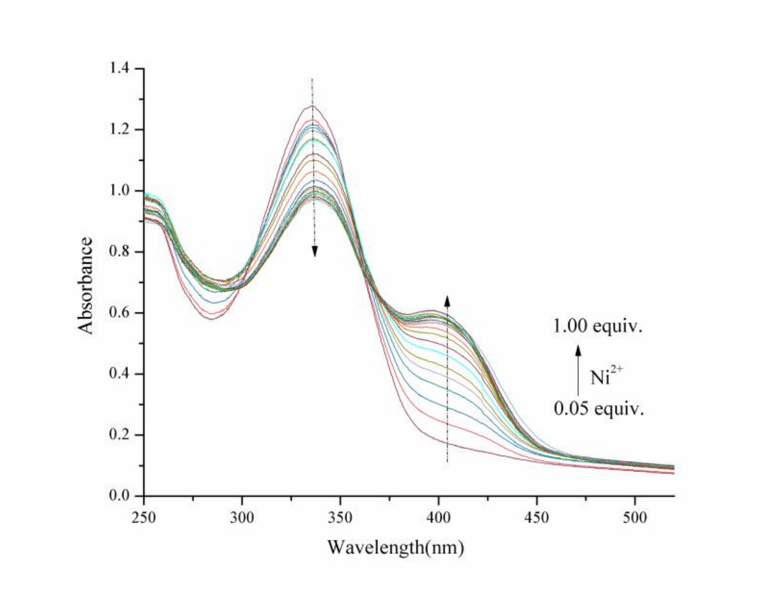

(b)

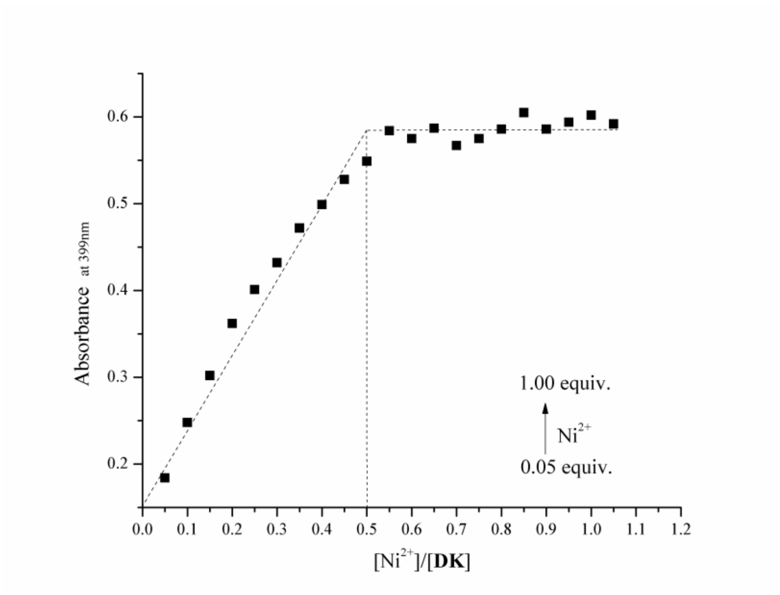

Figure S9 Job's Plot showing the 2:1 stoichiometry between **DK** and Ni^{2+}. (a) Absorption spectra of **DK** (1.0×10^{-5} M) in the presence of different concentration of Ni^{2+} (0.05-1.0 equiv.) in HEPES buffer /CH_3CN (0.01 M, pH=7.3, V/V = 10:90) solution. (b) A plot of absorption intensity depending on the concentration of Ni^{2+} in the range from 0.05-1.0 equiv.

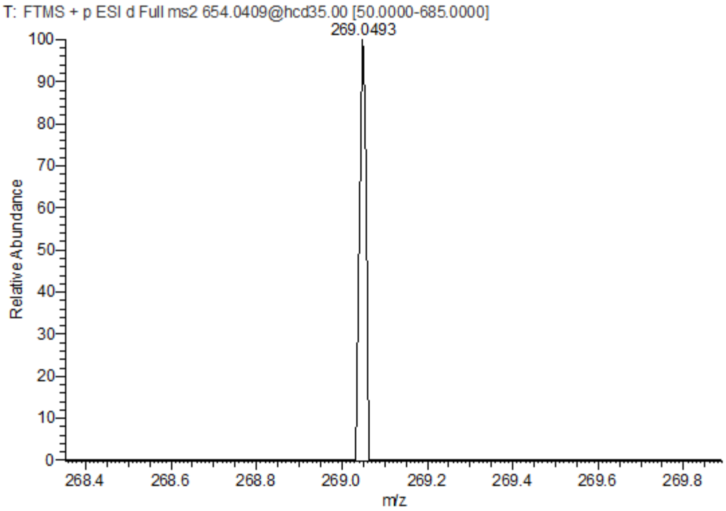

Figure S10 ESI-MS data of [**DK**-CN + H^+]$^+$.

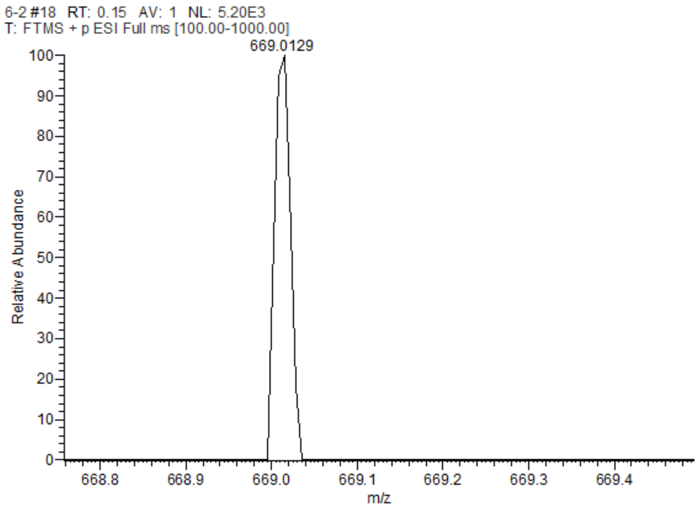

Figure S11 ESI-MS data of [**DK**+$2Ni^{2+}$+$2NO_3^-$+H^+]$^+$.

(a)

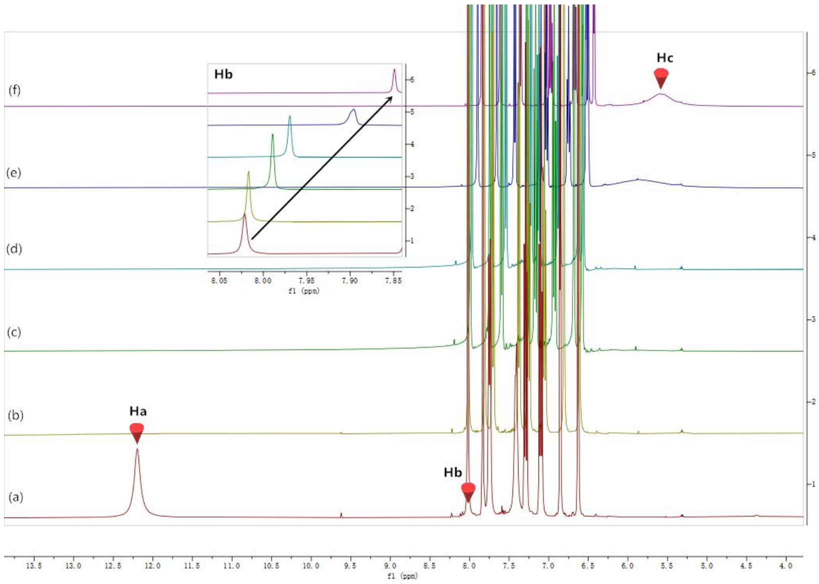

(b)

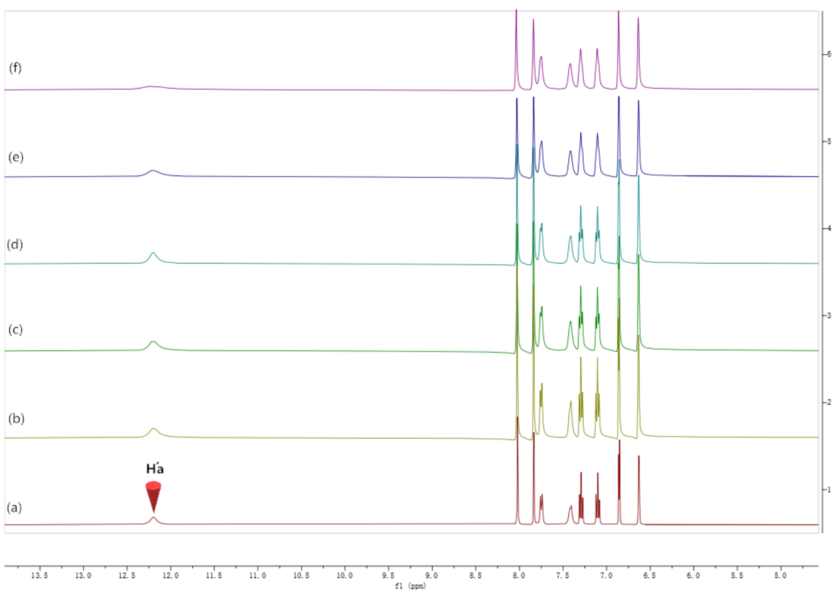

Figure 12 ^{1}H NMR titration spectra (DMSO-d_6, 400 MHz): (a) **DK** upon addition of CN^{-} (a-f: 0-1.5equiv.); (b) **DK** upon addition of Ni^{2+} (a-f: 0-0.75 equiv.).

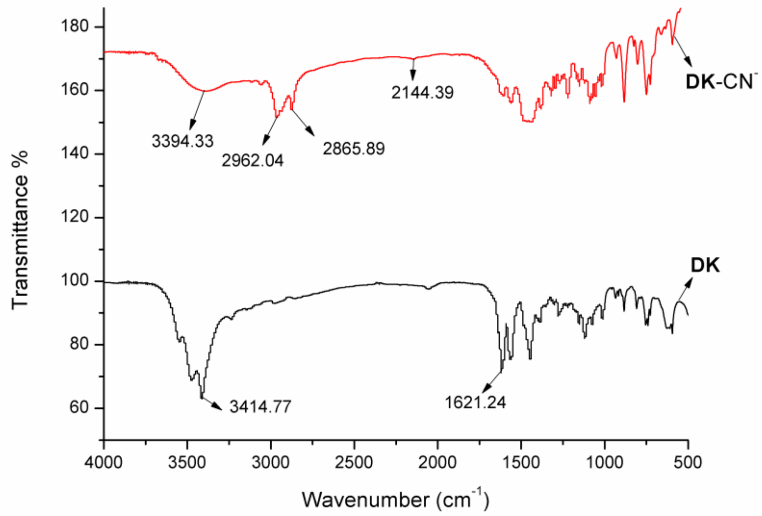

Figure S13 FT-IR spectra of **DK** and **DK** + CN^- in KBr disks.

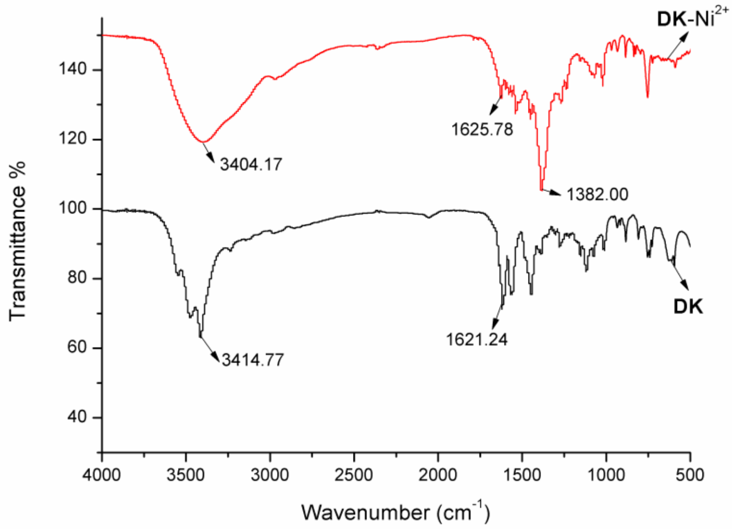

Figure S14 FT-IR spectra of **DK** and **DK** + Ni^{2+} in KBr disks.

The calculation of the detection limits (LOD):

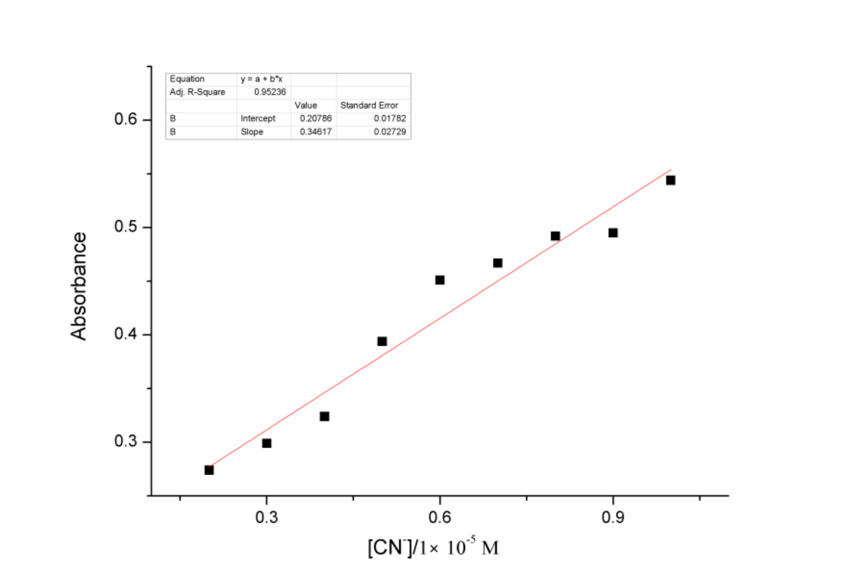

Figure S15 Detection limit of **DK** towards the detection of CN^{-}.

The linear equation was "y = 0.34617x + 0.20786".

According to the common equation "DL = 3δ/*k*" that the value of signal-to-noise ratio (S/N) was regulated at "3".

"δ" was the standard deviation of blank measurements (25 times detection). σ = 0.02

"*k*" represented the slope between absorbance versus the concentration of CN^{-}. $k = 0.34617 \times 10^{7}$

LOD = K × δ / S = 17×10^{-9} M.

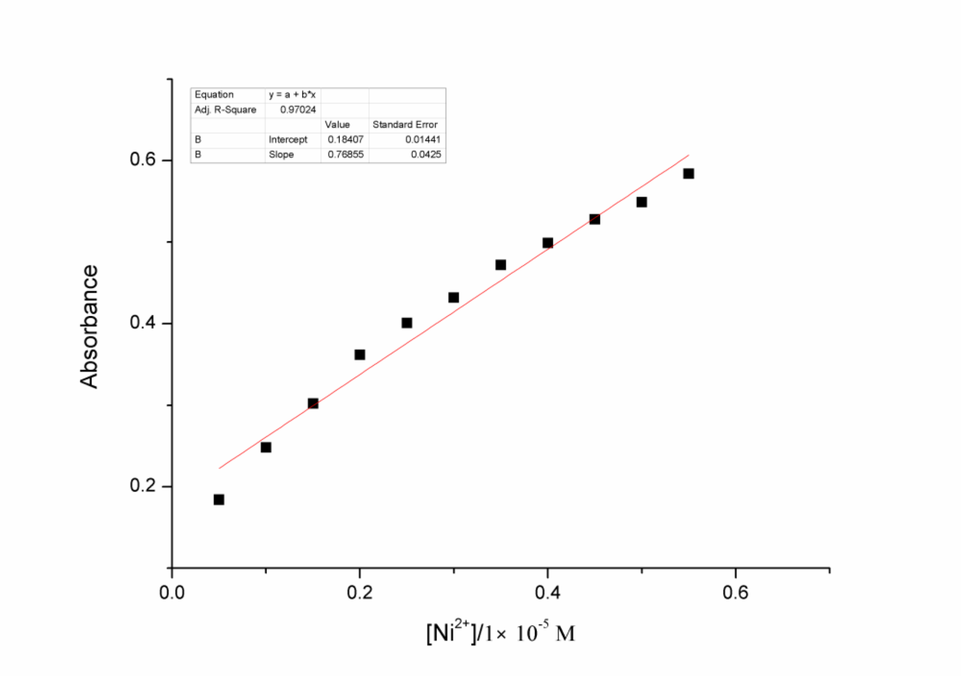

Figure S16 Detection limit of **DK** towards the detection of Ni^{2+}.

The linear equation was "y = 0.76855x + 0.18407".

According to the common equation "DL = 3δ/*k*" that the value of signal-to-noise ratio (S/N) was regulated at "3".

"δ" was the standard deviation of blank measurements (25 times detection). σ = 0.019

"*k*" represented the slope between absorbance versus the concentration of Ni^{2+}. $k = 0.76855 \times 10^7$

LOD = K × δ / S = 7.4×10^{-9} M.

Table S1 Comparison with the reported chemosensors with **DK**. The maximum allowable level of drinking water stipulated by the World Health Organization (WHO) were 1.9 μM for CN^- and 0.34 μM for Ni^{2+} [1, 2].

Chemosensor	Detected ion	Detection limit	Detection medium	Refs.
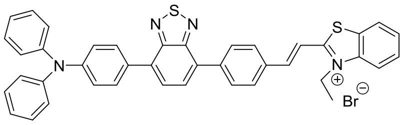	CN^-	1.34×10^{-7} M	THF/H_2O (2:8, v/v)	3
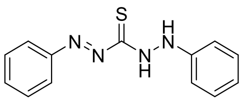	CN^-	4.8 $\times10^{-7}$ M	DMSO/H_2O (9:1, v/v)	4
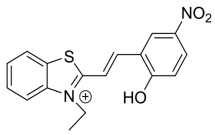	CN^-	1.8 $\times10^{-7}$ M	DMSO/H_2O solution (6:4, v/v, containing 0.01 M HEPES, pH 7.26)	5
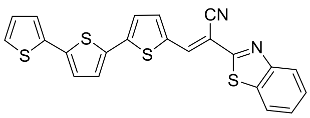	CN^-	4.6 $\times10^{-7}$ M	DMSO/H_2O (9:1, v/v)	6
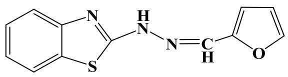	CN^-	17 $\times10^{-9}$ M	HEPES buffer /CH_3CN (0.01 M, pH=7.3, V/V = 1:9)	***Present work***
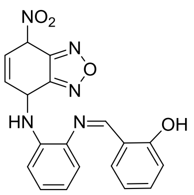	Ni^{2+}	1.1 $\times10^{-6}$ M	MeOH/H_2O 1 : 1, HEPES buffer, pH = 7.0	7
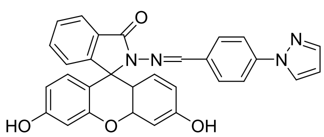	Ni^{2+}	2.61 $\times10^{-8}$ M	Ethanol	8
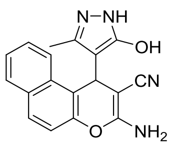	Ni^{2+}	1.91 $\times10^{-6}$ M	THF/H_2O (1.5:8.5, v/v)	9

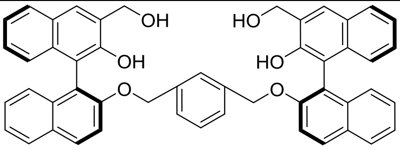	Ni^{2+}	4.91×10^{-6} M	MeOH/H_2O (1:1 (v/v), HEPES (50 mM), pH at 7.4	10
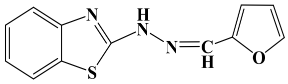	Ni^{2+}	7.4×10^{-9} M	HEPES buffer /CH_3CN (0.01 M, pH=7.3, V/V = 1:9)	***Present work***

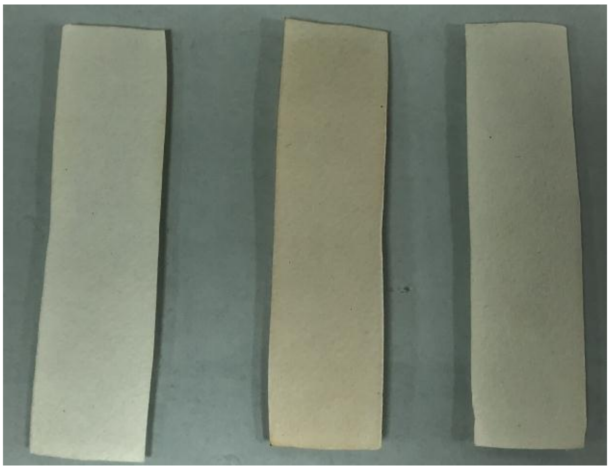

Figure S17. Test papers immersed in tap water contaminated with different contaminants, from left to right: the distilled water, the solutions of CN^- in tap water and the tap water.

References

[1] Amhed, F.; Chorus, I.; Cotruvo, J.; Cunliffe, D.; Endo, T.; Fawell, J. K.; Howard, G.; Jackson, P.; Kumar, S.; Kunikane, S.; Magara, Y.; Ohanian, E.; Ong, C. N.; Schmoll, O. Guidelines for Drinking-Water Quality, 3rd ed., World Health Organization, Geneva, Switzerland, 2004.

[2] Zhu, Y.; Wang, Z.; Yang, J.; Xu, X.; Wang, S.; Cai, Z.; Xu, H. J. N, N-Bis (2-pyridylmethyl) amine-based truxene derivative as a highly sensitive fluorescence sensor for Cu^{2+} and Ni^{2+} ion. *Chinese J. Org. Chem.*, 2019, **39**, 427-433.

[3] Zhai, B.; Hu, Z.; Peng, C.; Liu, B.; Li, W.; Gao, C. Rational design of a colorimetric and fluorescence turn-on chemosensor with benzothiazolium moiety for cyanide detection in aqueous solution. *Spectrochim. Acta. A.* **2019**, 224, 1117409-117415.

[4] Tavallali, H.; Deilamy-Rad, G.; Parhami, A.; Kiyani, S. Dithizone as novel and efficient chromogenic probe for cyanide detection in aqueous media through nucleophilic addition into diazenylthione moiety. *Spectrochim. Acta. A.* **2014**, 121, 139-146.

[5] Li, J.; Qi, X.; Wei, W.; Liu, Y.; Xu, X.; Lin, Q.; Dong, W. A "donor-two-acceptor" sensor for cyanide detection in aqueous solution. *Sensors Actuators B Chem.* **2015**, 220, 986-991.

[6] Niu, Q.; Lan, L.; Li, T.; Guo, Z.; Jiang, T.; Zhao, Z.; Feng, Z.; Xi, J. A highly selective turn-on fluorescent and naked-eye colorimetric sensor for cyanide detection in food samples and its application in imaging of living cells. *Sens. Actuators B: Chem.* **2018**, 276, 13-22.

[7] Rani, R.; Paul, K.; Luxami, V. An NBD-based two-in-one Cu^{2+}/Ni^{2+} chemosensor with differential charge transfer processes. *New J. Chem.* **2016**, 40, 2418-2422.

[8] Yang, G.; Meng, X.; Fang, S.; Wang, L.; Wang, Z.; Wang, F.; Duan, H.; Hao, A. Two novel pyrazole-based chemosensors:"naked-eye" colorimetric recognition of Ni^{2+} and Al^{3+} in alcohol and aqueous DMF media. *New J. Chem.* **2018**, 42, 14630-14641.

[9] Pannipara, M.; Al-Sehemi, A. G.; Irfan, A.; Assiri, M.; Kalam, A.; Al-Ammari, Y. S. AIE active multianalyte fluorescent probe for the detection of Cu^{2+}, Ni^{2+} and Hg^{2+} ions. *Spectrochim. Acta. A.* **2018**, 201, 54-60.

[10] Velmurugan, K.; Prabhu, J.; Raman, A.; Duraipandy, N.; Kiran, M. S.; Easwaramoorthi, S.; Tang, L.; Nandhakumar, R. Dual Functional Fluorescent Chemosensor for Discriminative Detection of Ni^{2+} and Al^{3+} Ions and Its Imaging in Living Cells. *ACS Sustain. Chem. Eng.* **2018**, 6, 16532-16543.